



Contents lists available at <http://qu.edu.iq>

Al-Qadisiyah Journal for Engineering Sciences

Journal homepage: <https://qjes.qu.edu.iq>



Rehabilitation of steel structures using innovative brace members equipped with YSPD damper

Wafaa Abbas Hasan * , Daniz abd alsajad baktash , and Alyaa Noori Gumar

Department of Civil Engineering, Faculty Of Technical Engineering And Agriculture, Islamic Azad University of Kermanshah, Iran

ARTICLE INFO

Article history:

Received 25 May 2024

Received in revised form 18 July 2024

Accepted 07 September 2024

Keywords:

Seismic energy

YSPD damper

Passive energy dissipation device Each

Numerical research

Brace member with damper

Brace member with out damper

ABSTRACT

Earthquakes are serious risks to human life and infrastructure. An earthquake's influence on human life and its socioeconomic consequences highlight the need to investigate and create the most efficient and easily adaptable ways for minimizing losses. The basic concept of different control mechanisms used for protecting structures from the destructive impacts of earthquakes is to dissipate the energy efficiently, therefore ensuring that the structure remains undamaged or sustains minimum damage. To achieve this purpose, the passive control mechanism is a particularly suitable and reliable technology as it doesn't rely on external power to actively dissipate energy. The present study proposes using a passive energy dissipation device called the Yielding Shear Panel Device (YSPD) for strengthening the current steel structures. The YSPD consists of a square hollow section (SHS) that houses a diaphragm plate. The fundamental concept of the YSPD involves harnessing the lateral deformation of a steel plate to absorb and disperse the seismic energy. The Bouc-Wen-Baber Noori (BWBN) material has been used for simulating the hysteresis force-deformation relationship of YSPDs by pinching. YSPDs are simulated as spring components that connect between the beam and the V-brace. A nonlinear time history dynamic analysis was performed to assess the alteration in the structural capacity with the setting up of YSPDs. The performance of the tested structure was assessed considering story drift, story displacement, story shear, column shear, and YSPD hysteresis loops. The results indicated that YSPD installation has improved the structure's capacity. However, the use of dampers resulted in significant drift in all stories, a reduction in total floor displacement, and a decrease in the shear force of the stories. However, the results demonstrated that the YSPD dampers effectively absorbed energy and exhibited stable hysteresis loops.

© 2024 University of Al-Qadisiyah. All rights reserved.

1. Introduction

Current catastrophic seismic events in numerous areas of the world highlight the effect of this unforeseen phenomenon on human civilization and indicate the need for more study to identify sustainable solutions to reduce the resulting loss. Over the same time period, researchers developed various types of active, semi-active, and passive energy dissipation technologies that reduce damaging seismic effects. Passive energy dissipating systems are cheaper and easier to set up, as well as may efficiently reduce the damaging effects of earthquakes, while these tools don't need a power supply compared to active energy dissipation systems.

Numerous passive control systems developed in the previous few years that exploit the yielding of metal plates to dissipate energy, such as the added damping and stiffness (ADAS) device [1-3], the triangular added damping and stiffness (TADAS) device [4,5], and the steel plate shear wall (SPSW) [6,7], among others. These metal-yielding devices use the component materials' stable hysteretic reaction to dissipate energy.

The Yielding Shear Panel Device (YSPD) [8, 9] is a newly developed metal-based energy dissipation device, as shown in Figure 1. YSPD is highly easy to construct and economical, especially compared to existing

* Corresponding author.

E-mail address: Wafaahassan762@gmail.com (Wafaa Abbas)



devices. This device was first presented by Williams and Albermani [10] and was based on a design that U. Dorka of the University of Kassel, Germany, had suggested for taking advantage of the energy dissipative capacity of steel plates through in-plane shear deformation, and the proposal was then developed by Schmidt et al. [11] and Williams and Albermani [8]. YSPD depends on the in-plane shear deformation of a square hollow section (SHS), which has a thin diaphragm steel plate welded inside of it. Chan et al. [9] presented an analytical model for YSPD, assuming the shear plate was simply supported. The square section is more efficient in creating a 45° tension field compared to the rectangular section [9]. The steel diaphragm plate is welded within the square hollow section, and it deforms in shear to release earthquake energy as a result of the relative horizontal displacement of the top and bottom portions of the section. This device can be installed under a structural beam utilising a V-brace such that it activates automatically in case of any horizontal excitation. Deformed shape and schematic diagram illustrating the geometric parameters of YSPDs are illustrated in Figure 1(b and c). A number of studies were previously conducted to identify the range of possible shear deformations. According to the investigations [12], the shear deformation angle of SPD exceeds 0.05 under cyclic loading, which is about 30 times more than the shear yield deformation angle. For monotonic loading, the shear deformation angle is greater than

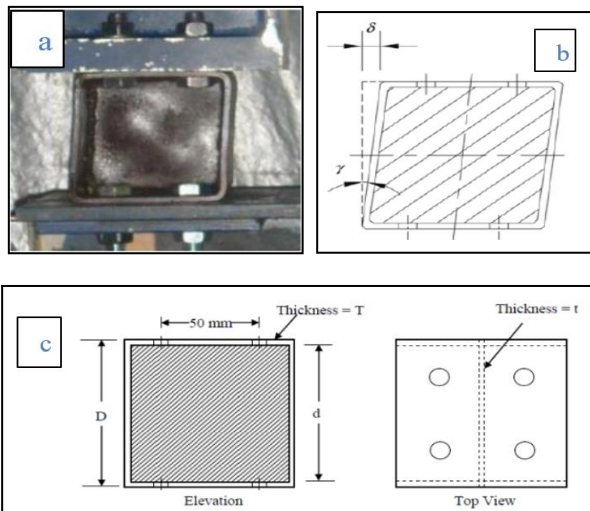


Figure 1. (a) Yielding shear panel device (b) Deformed Shape (c) Schematic diagram showing the geometric parameters of YSPDs [15]

0.1. Hossain et al. [13] examine the evaluation of efficiency in order to assess the suitability of YSPDs (yielding steel plate devices) in the presence of uncertainties such as earthquakes, material strength, stiffness, and structural reaction. They also analyze performances by considering YSPDs' size, number, and arrangement. Kim et al. [14] performed shake table tests on a steel shear panel and observed that the relative displacement corresponds to a drift ratio of 0.0276. As a result, it appears that performing numerous seismic tests on frame structures to assess the effectiveness of YSPD devices and their design parameters is time-consuming. Thus, numerical modelling offers a different technique for estimating a YSPD's deformation capacity and calculating its cumulative dissipated energy.

Finite element methods (FEMs) are commonly used for analyzing the mechanical characteristics of steel panels. Chan et al. [16] evaluate the

seismic performance of perforated yielding shear panel device (PYSPD). The finite element model demonstrated the development of a tension field due to shearing action [17-18]. Furthermore, the PYSPD resulted in a reduction in elastic stiffness and yield strength, thereby establishing a stable and predictable hysteretic behavior. Hossain et al. [19] created a finite element model for YSPD using the ANSYS finite element software. Their emphasis was on modelling suitable support conditions, initial geometric defects, and residual stresses. They found that theoretical predictions for monotonic loading exhibited a high degree of similarity with both the finite element (FE) analysis and the experimental results. Zhengying et al. devised a modelling method that accurately represented the hysteretic behaviour of YSPD [20]. Using Simulink, they designed a BWBN model of the YSPD that considers pinching and calibrates the hysteretic parameters; they applied experimental data of the YSPD. This work utilized six different types of specimens. They demonstrated that the energy dissipation of YSPD is 10% lower when compression is included in the model. The addition of pinching provided better agreement with the test results for both of the specimens. Hossain et al. 2012[21] proposes a mathematical model to predict the hysteretic response using easily available parameters, i.e. the geometry of the YSPD and the properties of the material. This proposed mathematical formulation will allow evaluating YSPDs performance in energy absorption through simulation as well as to develop design methods to identify appropriate size, location and numbers of YSPDs that are required for seismic retrofitting. Similar studies were also observed in [8, 22-24]. According to the above-mentioned literature, the computing resources and effort required to perform reliability analysis in finite element program ABAQUS, DIANA, or ANSYS software are significant and reduce the possibility of using either software package in this application. Open System for Earthquake Engineering Simulation (OpenSees) is a numerical program and object-orientated software that was primarily developed at the University of California, Berkeley, for the nonlinear analysis of structures during seismic loadings [25]. OpenSees has primarily focused on developing an effective computational tool for evaluating the nonlinear behaviour of structural frames under seismic excitations. This study aims to investigate the rehabilitation of steel structures using innovative brace members equipped with YSPD dampers. For this purpose, we used the FE modeling technique, specifically the FE package OpenSees, to model the North-South lateral load-bearing frame of the three-story Los Angeles SAC structure as a 2-dimensional frame. It also did a time-history dynamic analysis to see if YSPDs could be used to retrofit steel structures and tested how well the frames worked with these yielding dampers when they were subjected to different earthquake intensities, frequency compositions, and lengths. The former was achieved through story drift, story displacement, story shear, column shear, and the YSPD hysteresis loop.

2. Description of the building

The moment-resisting frame of the Los Angeles (LA) three-story SAC model structure, which was constructed for the SAC Phase II Steel Project [26-27], has been utilized by numerous researchers to assess the performance of a variety of seismic control devices [28-30]. The current research focusses on the Boston 3-story buildings, which are known as BO3. The structure has been designed according to the pre-Northridge codes (UBC 1994). During the design of the building, the external frames were designed to resist the lateral seismic loads, and the interior frames were designed as gravity frames. Seismic load considerations controlled the

lateral load design of the LA structure. The study frame consists of three stories each 3.96 m high, four equal bays of 9.15 m wide, and six equal bays of 9.15 m length (see Figure 2). The design yield strength of the beams and girders is $f_y = 248.211$ MPa (36 ksi), of the columns is $f_y = 344.7$ MPa (50 ksi) are used. Also, 36-grade steel for beams and girders was used. Many of the girder sizes are controlled by drift instead of strength considerations. Table 1 summarises the beam and column sections of the North-South lateral load-bearing frame. The proposed structure for evaluating the performance of YSPD was a four-bayed North-South lateral load-bearing moment-resisting frame. The location of the moment resisting frames is shown by the bold lines in Figure. All the columns in the perimeter moment frames bend about the strong axis. The strong axis of the gravity frame columns' is orientated in the NS direction. Figure 3 shows the floor plan and the moment-resisting frame of the three-story SAC model structure.

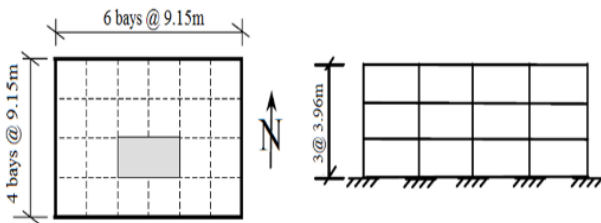


Figure 2. Floor Plan and Elevation for Model Building

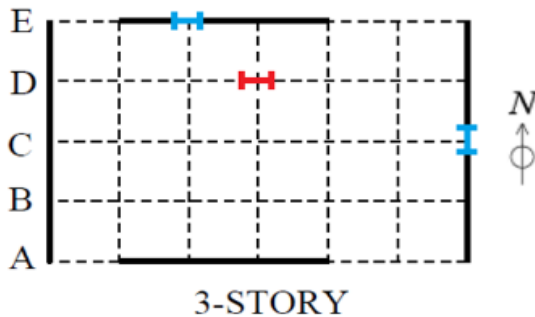


Figure 3. Floor Plan Layout of Moment Resisting Frames for BO Model Building

Table 1. Beam and Column Sections for Boston Model Building “NS Moment Resisting Frame (3-story Building)”

Story/Floor	Columns		Doubler Plates (in)	Girder
	Exterior	Interior		
1/2	W14X74	W14X99	0,0	W18X35
2/3	W14X74	W14X99	0,0	W21X57
3/Roof	W14X74	W14X99	0,0	W21X62

NS Gravity Frames			
	Columns		Beams
	Below penthouse	Others	
	4-W12X65 & 2-W12X72	W12X58	W16X26
	4-W12X65 & 2-W12X72	W12X58	W16X26
	4-W12X65 & 2-W12X72	W12X58	W14X22

3. YSPD damper

YSPDs are utilized in the moment-resisting frame to dissipate earthquake energy by shear deformation. Geometry nonlinearity is implemented into the modelling of YSPD to analyse the post-buckling behaviour of YSPD. The primary buckling mode of deformation is employed as the initial geometric imperfection. The initial buckling deformation was performed at an amplitude of $0.2t$, where t represented the thickness of the diaphragm plate. The deformation was scaled as a function of plate thickness. The detailed modelling and connection of the YSPD with the steel base plate are provided by Hossain et al. [18].

YSPDs are installed in the North-South lateral load-bearing moment-resisting frame of the SAC three-story building to enhance its seismic resistance. YSPDs are installed on every storey of one interior bay, as illustrated in Figure 4, and in all moment-resisting bays. The current study, as illustrated in Table 2, incorporates three different types of bracings and three different sizes of YSPDs. Cold-formed, welded Hollow Structural Sections (HSS) are implemented as the strengthening system. HSS is made up of ASTM A500 Grade B steel. The seismic energy will be absorbed and dissipated by the inelastic shear deformation of the diaphragm plate. The addition of the V-brace system will enhance the structural rigidity, resulting in an increase in the elastic stiffness of the building's floors until the response of the Yielding Strength Point Displacement (YSPD) becomes plastic.

Table 2. Brace size utilized in the present study.

YSPD	Steel brace
YSPD 100x4x2	HSS 4x4x1/8
YSPD 110x5x3	HSS 4x4x1/4
YSPD 120x6x4	HSS 4x4x1/2

4. Numerical models in OpenSees

4.1 Structural model

OpenSees software models the North-South lateral load-bearing frame of the three-story Los Angeles SAC structure in two dimensions [31]. The slab system is supposed to be sufficiently rigid to preclude lateral movement in the frame's normal direction. The far end simply supports beams, while the columns are modeled as elastic beam-column components. The connecting elements between the column joints and simply supported beams, which used zero-length springs with negligible stiffness. Fixed supported beams are represented as elastic beams with hinges. These designs used the typical beam-to-column welding connection features. Figure 4 illustrate the Analytical model of the North–South lateral load-bearing moment resisting frame equipped with YSPDs. Appendix A presents an extensive description of the incremental algorithm and BWBN model for OpenSess implementation.

The design offices use perimeter moment-resistant frames as their preferred structural system. As the interior frames are classified as gravity frames, each lateral load-bearing frame is responsible for carrying half of the seismic load. A mix of distributed load and point load imposes the seismic force on the frame. A distributed load was applied to the beams depending on the surrounding East-West Bay's tributary region. The remaining seismic load acts as a point load for an artificial gravity column, also known as a "leaning column." Rigid links are used to pin-connect the dummy column with the lateral force-resistant frame. Rigid links are used

to pin-connect the dummy column with the lateral force-resistant frame. The dummy column is simulated as an elastic beam-column element with a high axial and bending stiffness, and a hinge with negligible rigidity is used at the beam extremities to simulate a similar moment release as rigid links.

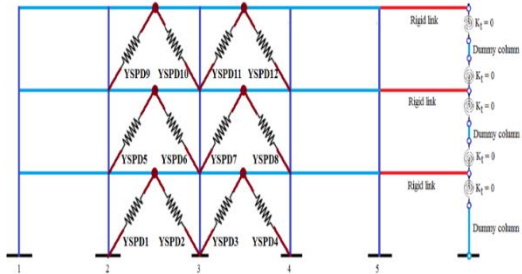


Figure 4. Analytical model of the North–South lateral load-bearing moment resisting frame equipped with YSPDs.

4.2 Material modeling for YSPD

For strengthening the building against seismic loading, YSPDs (passive energy devices) are utilized in the moment-resisting steel frame when combined with V-bracing. YSPD is installed in a framed structure that supports a beam via an inverted V-brace connection [32]. The Bouc-Wen-Baber Noori (BWBN) model is employed to illustrate the pinching hysteretic force deformation relationship of YSPDs [33]. In order to develop a nondegrading pinching hysteretic BWBN model, two different types of parameters are employed: hysteretic parameters and pinching parameters. The force-displacement curve's shape is represented by the hysteretic parameters, while the pinching effect is illustrated by the pinching parameters. The BWBN model parameters of YSPD are illustrated in Table 3. When evaluating seismic performance, we consider only one YSPD size (YSPD 100x4x2); see Table 3.

Table 3. Material parameters for the YSPDs by BWBN [34].

YSPD (D×T×t)	100x4x2	110x5x3	120x6x4
F _y (Mpa)	0250	300.0	350.0
K _t (KN/mm)	00.33	00.42	00.49
F _i (KN)	26.76	54.22	93.51
A	0001	00001	0001
β	00.50	00.50	00.50
γ	00.50	00.50	00.50
n	1.213	00.54	00.30
ξ ₁₀	00.96	00.95	00.95
P	00.18	00.15	00.12
Ψ ₀	00.41	00.27	00.22
δ _ψ	0.00001	0.00001	0.00001
λ	00.03	0.0014	0.0002
q	00.52	00.38	00.30

[Ⓜ]D is the Size of YSPD (mm), T is the thickness of SHS plate (mm), t is the thickness of diaphragm plate (mm). K_t is the tangential stiffness of YSPD after tension field formation (kN/mm). A, γ, β, n are hysteretic parameters and q, ξ₁₀, ρ, ψ₀, δψ, λ are pinching parameters. F_y is the yield strength of SHS and diaphragm plates.

Hossain and Ashraf [23], as well as Figure 5, illustrate the force displacement formulas for the appropriate YSPDs. The YSPDs are

simulated as a spring element that is connected to the midspan of the beam and the V-bracing. The braces were created for preserving their elasticity by respecting a design force of 2F_i.

4.3 Fiber element

The fiber model's basic idea is to divide the element section into specific small components, as indicated by the term "fiber". To enhance the handling of biaxial bending coupling with axial force, we can calculate the overall section's stress-strain relationship based on the fiber's uniaxial stress-strain relationship. The fiber model method allows us to calculate the stiffness matrix along the longitudinal division of each structure element using n integration points. Figure 6 illustrates the division of each integration point into multiple fibers. Provided that the constitutive model of materials is accurate and there are sufficient cross-section subdivisions, calculation accuracy can be achieved.

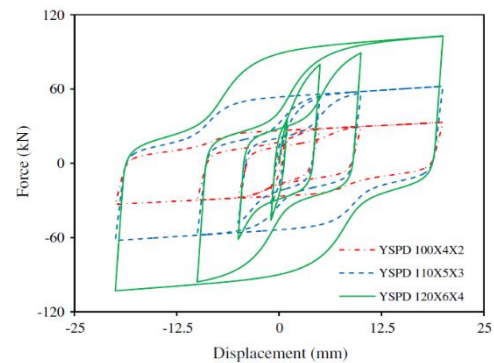


Figure 5. Relationship between the YSPDs' cyclic force displacement use the BWBN simulations [7]

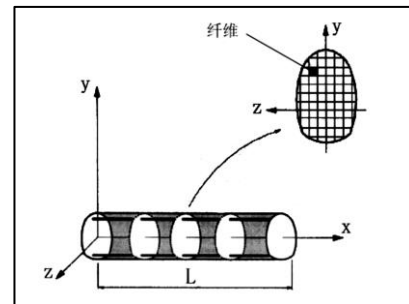


Figure 6. The fiber element in local coordinates [35]

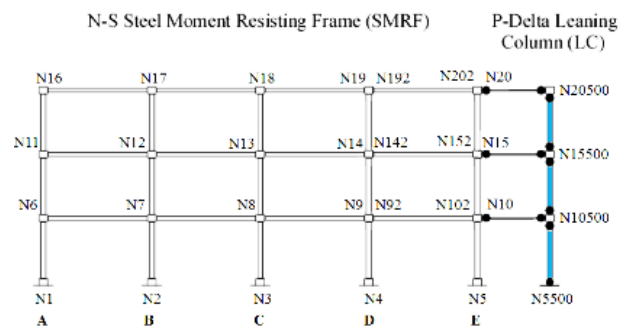


Figure 7. Numbering of frame nodes (centerline of sections).

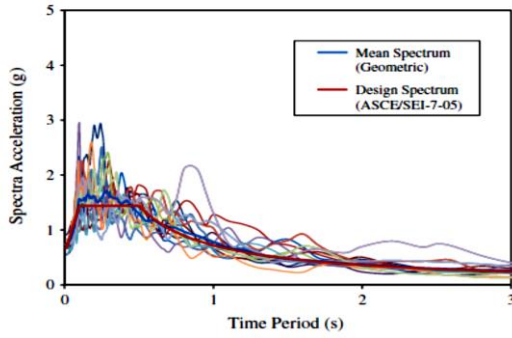


Figure 8. Response spectrum of the normalized ground motion data and design response spectrum at central Los Angeles for this location class D (rigid soil).

Different uniaxial constitutive models could be assigned to the fibers for the same material, which exhibit distinctive mechanical behavior as a result of varying lateral restraints, including those from a stirrup, steel tube, and carbon fiber sheet. Figure 7 illustrates the numbering of frame nodes (centerline of sections). Table 4 shows the coordinates of model nodes. Therefore, we employ OpenSees v1.7.2 to conduct an inelastic 3D time history analysis of the steel frame.

Table 4. Coordinate of model nodes

Node	xCrd(m)	yCrd(m)	Node	xCrd(m)	yCrd(m)
01	00.00	0.00	00011	00.00	07.92
02	09.15	0.00	00012	09.15	07.92
03	18.30	0.00	00013	18.30	07.92
04	27.45	0.00	00014	27.45	07.92
-	----	----	00142	27.45	07.92
05	36.60	0.00	00015	36.60	07.92
-	-----	-----	00152	36.60	07.92
5500	54.75	0.00	15500	54.75	07.92
06	00.00	3.96	00016	00.00	11.88
07	09.15	3.96	00017	09.15	11.88
08	18.30	3.96	00018	18.30	11.88
09	27.45	3.96	00019	27.45	11.88
92	27.45	3.96	00192	27.45	11.88
10	36.60	3.96	00020	36.60	11.88
102	36.60	3.96	00202	36.60	11.88
10500	54.75	3.96	20500	54.75	11.88

4.4 Seismic modeling

Time history analysis is an extremely effective method for producing dynamic scenes of seismic devastation that are acceptable [9]. In recent years, many researchers have frequently employed the time history analysis technique to determine the seismic vulnerability of various structures [36-37]. This study performed a nonlinear time history analysis of five distinct earthquake recordings, which included fault normal and fault parallel earthquake values for each earthquake. Table 5 presents the earthquake records. On the other hand, the time history analysis has been conducted for twenty earthquakes, which is compatible with the design.

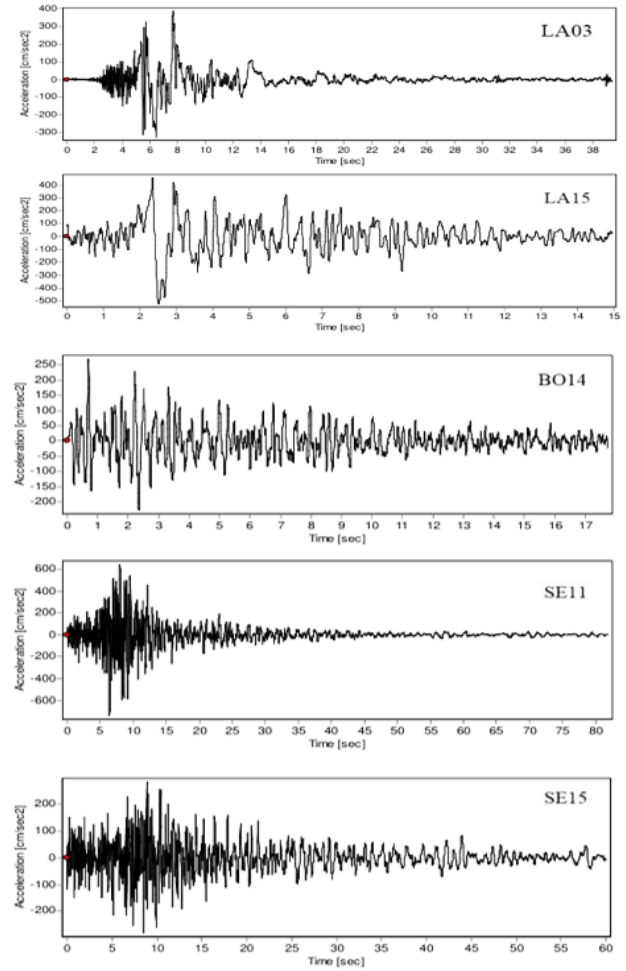


Figure 9. Earthquake record for variety SAC building.

Table 5. Details of considered Ground Motion (Having a probability of Exceedance of 10% in 50 Years)

SAC Name	Record	Earthquake Magnitude	Distance (km)	Duration (sec)	PGA (cm/sec ²)
LA03	Imperial Valley, 1979, Array #05	6.5	4.1	39.38	386.04
LA15	Northridge, 1994, Rinaldi RS	6.7	7.5	14.945	523.30
BO14	Saguenay, 1988	5.9	96	17.735	284.44
SE11	Puget Sound, Wa., Olympia, 1949	7.1	80	81.82	737.82
SE156	Eastern Wa., Tacoma County, 1949	7.1	60	59.98	284.72

Figure 8 illustrates the response spread of the normalized ground-motion data and the design response spectrum for the location of class D in central Los Angeles. Analysis was performed on the ten different kinds of frames, and the results were compared. The results show that the time periods have decreased as the number of YSPDs has increased. Figure 9 shows the earthquake recorded for five building.

5. Seismic analysis results

After dynamic analysis of all models in OpenSees software, the demand responses of considered structures (retrofitted structure and bare frame) have been evaluated from different aspects.

5.1 Story drift

One of the most important responses of structures in an earthquake is the understory drift response. Drift measures the bending of columns and the failure of elements that are susceptible to displacement within the structure's stories. Figures 10 to 15 show the maximum drift value recorded for frame stories in BO14 and SE15 earthquake records, as well as at different intensities. It's important to note that distinct stories record their maximum drift at distinct times, not simultaneously. However, this graph only shows the maximum drift values. Figures 10-12 show that for the bare frame, the interstory drift demand is higher at the third-floor level than the other two floor levels, and it is also true for BO14 earthquakes. For SE15 earthquakes, the intersecondary drifts of the structure are larger than the other stories, as seen in Figures 13-15.

As can be seen in these figures, in all earthquake intensities, the use of dampers has effectively helped to reduce interstory drift ratio. Figures 10 to 15 show that for both BO14 and SE15 earthquakes, the interstory drift demand has decreased after installing the YSPDs in the first and third stories, but it has increased largely in the second story. However, lower intensities were associated with the greatest drift reduction.

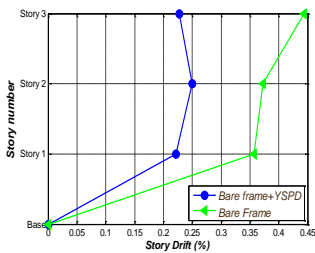


Figure 10. Maximum interstory drift of stories under BO14 earthquake and PGA=0.2g

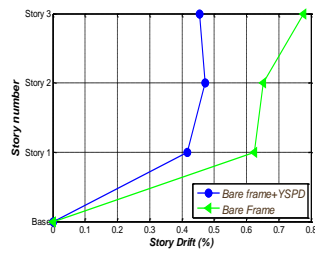


Figure 11. Maximum interstory drift of stories under BO14 earthquake and PGA=0.35g

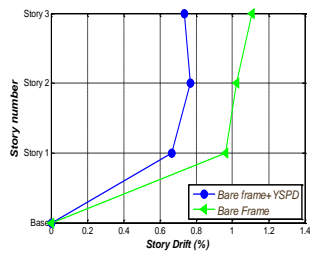


Figure 12. Maximum interstory drift of stories under BO14 earthquake and PGA=0.55g

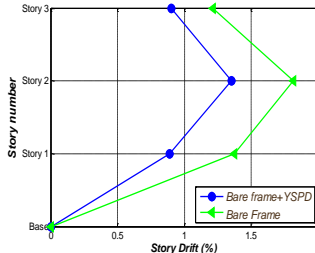


Figure 13. Maximum interstory drift of stories under SE15 earthquake and PGA=0.2g

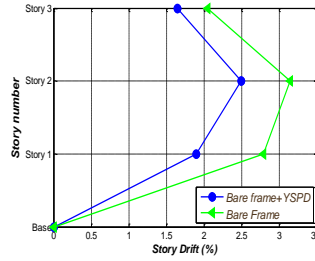


Figure 14. Maximum interstory drift of stories under SE15 earthquake and PGA=0.35g

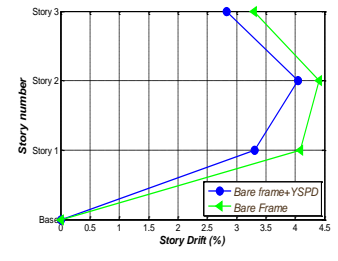


Figure 15. Maximum interstory drift of stories under SE15 earthquake and PGA=0.55g

Also, at higher intensities, dampers have played a more effective role in reducing drifts. Based on the comparison, it can be said that OpenSees properly predicts the moment of collapse and the deformation of the structure, as well as accurately simulates the reaction of the structure under extreme ground motion.

5.2 Story displacement

One of the other responses that is important in the seismic behavior of buildings is the total displacement of floors. Unlike drift, which is the deformation of each story and is calculated from the displacement of each floor relative to its lower floor, the total displacement is measured from the calculation of the displacement of each floor relative to the base level of the structure (ground level). This response is important in estimating the secondary effects of deformations (P-Delta effects) as well as investigating the possibility of buildings ponding. Figures 16 to 21 show the maximum amount of total displacement on different floors of the structure under LA15 and SE15 earthquake records, as well as at different earthquake intensities.

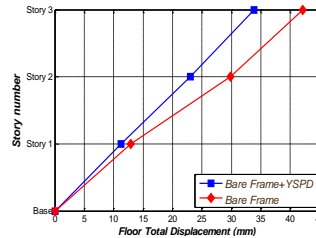


Figure 16. Floors maximum displacement under LA15 earthquake and PGA=0.20g

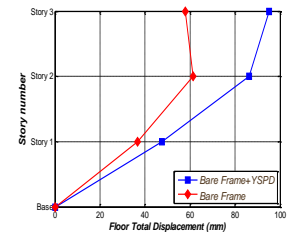


Figure 17. Floors maximum displacement under LA15 earthquake and PGA=0.35g

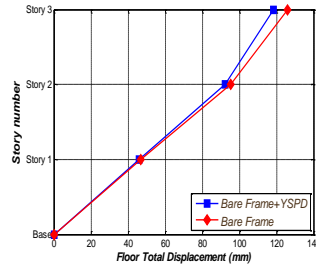


Figure 18. Floors maximum displacement under LA15 earthquake and PGA=0.55g

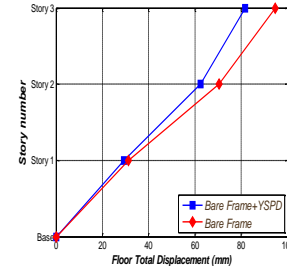


Figure 19. Floors maximum displacement under SE11 earthquake and PGA=0.20g

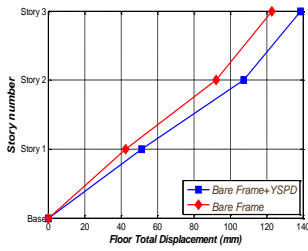


Figure 20. Floors maximum displacement under SE11 earthquake and PGA=0.35g

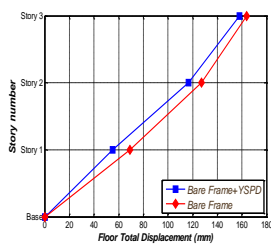
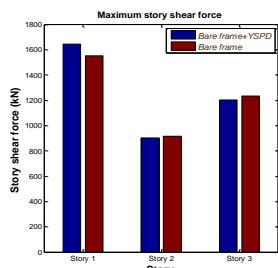


Figure 21. Floors maximum displacement under SE11 earthquake and PGA=0.55g

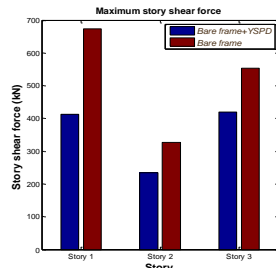
The use of dampers has effectively reduced the total displacement of floors. However, the effect of dampers in reducing displacement responses has been less than their effect in reducing drift responses.

5.3 Story shear

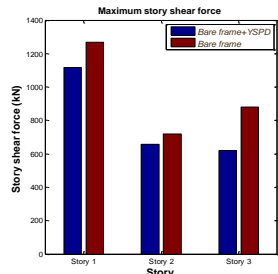
One of the other responses that is so vital in the seismic behavior of a structure is the shear force of the stories. The shear force of a story is actually the total lateral force demand in that story, which is obtained from the sum of the shear force in the columns and the horizontal force component endured in the braces (dampers in this study). Figures 22-24 compare the maximum shear force of the stories in the retrofitted structure and the bare frame under various earthquake conditions and intensities. As can be seen, except in one earthquake record (LA15), where the story shear force has increased in the first story, in other earthquake records and in different earthquake intensities, the story shear force in the retrofitted frame has mostly decreased in contrast to the bare frame. While the reduction in story shear force is not statistically significant, it is nonetheless a significant improvement. The reason for this is that the use of yielding dampers, such as ADAS and TADAS dampers, primarily increases the stiffness of the structure.



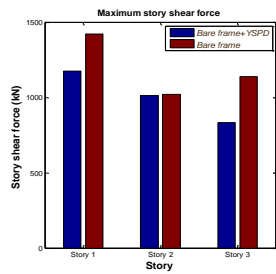
(a) Earthquake record: LA15



(b) Earthquake record: BO14

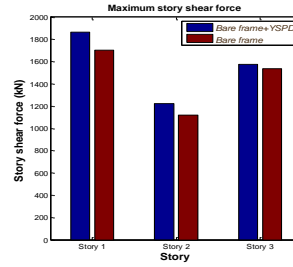


(c) Earthquake record: SE11

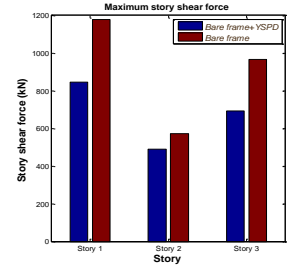


(d) Earthquake record: SE15

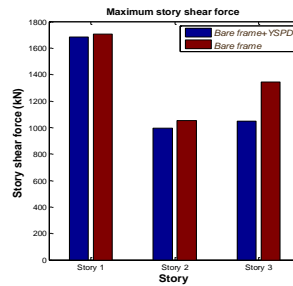
Figure 22. Maximum story shear force under different earthquakes with PGA=0.2g



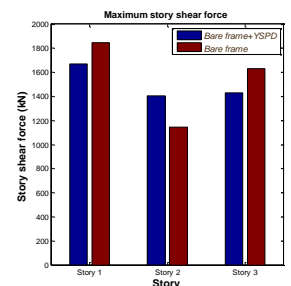
(a) Earthquake record: LA15



(b) Earthquake record: BO14

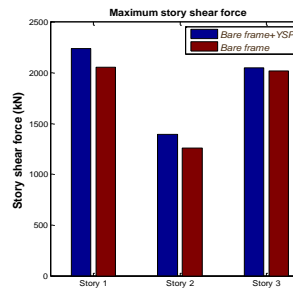


(c) Earthquake record: SE11

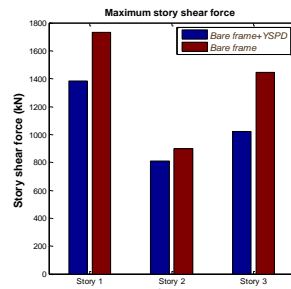


(d) Earthquake record: SE15

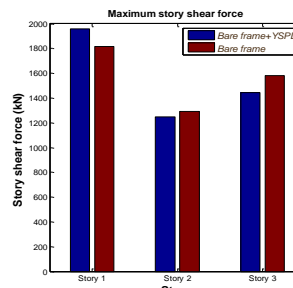
Figure 23. Maximum story shear force under different earthquakes with PGA=0.35g



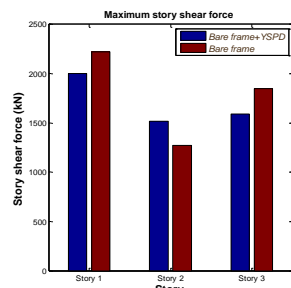
(a) Earthquake record: LA15



(b) Earthquake record: BO14



(c) Earthquake record: SE11



(d) Earthquake record: SE15

Figure 24. Maximum story shear force under different earthquakes with PGA=0.55g

This, in turn, increases the absorption of more seismic force in the structures, which is considered a disadvantage of their use. However, one advantage of shear-yielding dampers is their ability to help reduce the shear force of the stories.

5.4 Columns shear

As previously mentioned, the columns absorb part of the shear force of the stories, while the installed braces (dampers) absorb another part. A

point to consider is whether or not we have been able to reduce the amount of shear force in the columns by installing dampers. It should be mentioned that columns are also responsible for gravity load, and decreasing the shear and bending internal forces in them is an important issue. Therefore, in this section, we calculate the shear force of the columns in the retrofitted frame separately and compare it with the shear force of the columns in the bare frame to better check the changes in the columns' shear force by using YSPD dampers. Figures 25 to 27 illustrate the maximum values of the total shear force for the columns in both the retrofitted frame and the bare frame, under various earthquake conditions and intensities. In most cases, the retrofitted frame's columns have experienced a lower shear force compared to those in the bare frame, demonstrating a very favorable performance. As mentioned earlier, in the retrofitted structure, a part of the shear force of the story will not be absorbed by the columns and another part is absorbed by the dampers. For a better evaluation, in Figures 28 to 30, the contribution of columns and the contribution of dampers to the total shear force of stories are shown separately for different earthquakes and at different intensities. As can be seen, in all cases, a part of the shearing force has been absorbed by the braces, and this will reduce the role of the columns to absorb the shear forces. However, the contribution of dampers is not very high compared to columns. The reason for this performance can be related to the angle of placement of the braces in the frame. In fact, if the braces were placed more horizontally, we would see better performance of them for absorbing shear forces. Therefore, it is recommended that the braces place more horizontally, and on the other hand, they should be used in larger spans. In another proposal, they can be implemented in the form of concentrically X braces in the structure so that their angle to the horizon direction decreases and they show better performance.

Another important issue in evaluating dampers' performance is their hysteresis behavior. As previously mentioned, this study utilized the BWBN model to simulate the behavior of shear yielding dampers (YSPDs). This model effectively accounts for pinching phenomena in the software modeling of these dampers, and its outcomes align well with both experimentally tested models and finite element models from prior research. Figures 31 to 36 show the hysteresis curves of the force displacement of the YSPD dampers in BO14 and SE11 earthquakes, as well as at different intensities of the earthquakes. The area under these curves shows the energy absorbed by these dampers, and the larger area indicated that the damper has been able to dissipate a greater amount of seismic input energy. These diagrams demonstrate the effective absorption of energy in all stories by these dampers, along with their stable hysteresis loops, a crucial aspect of their behavior.

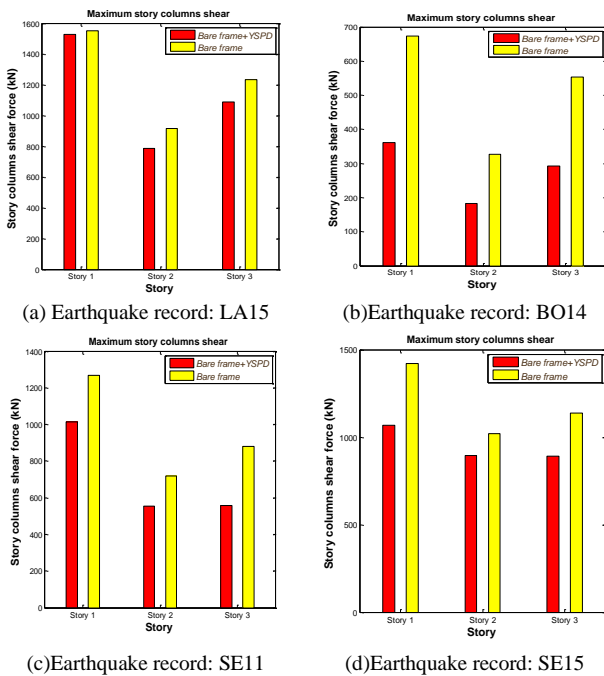


Figure 25. Maximum of columns shear under different earthquakes with PGA=0.20g

5.5 YSPD hysteresis loops

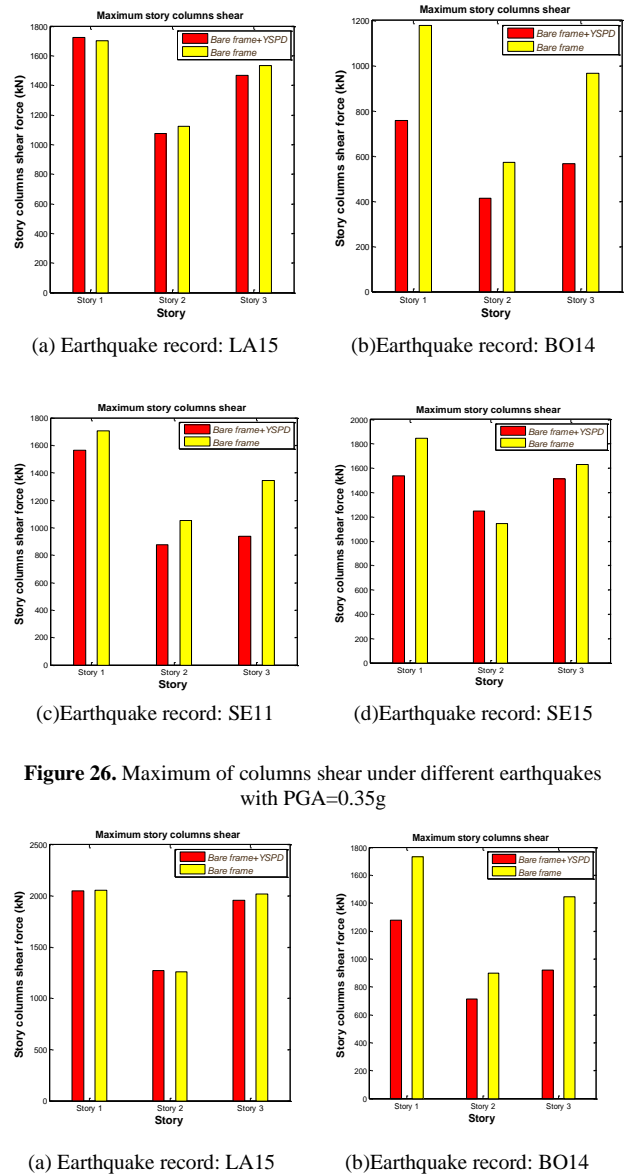
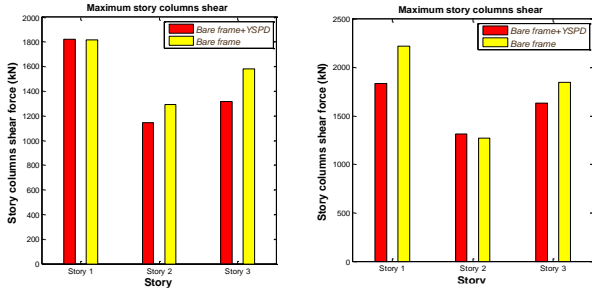
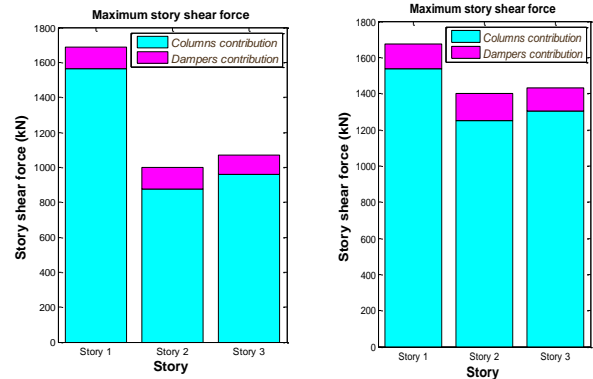


Figure 26. Maximum of columns shear under different earthquakes with PGA=0.35g

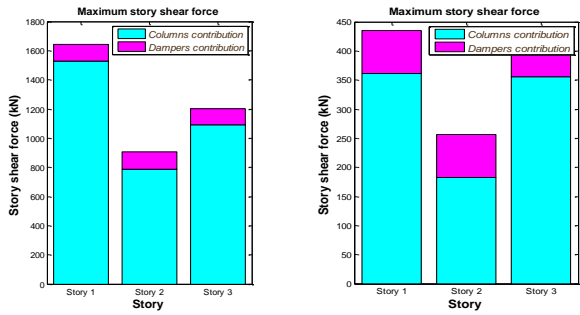
Figure 27. Maximum of columns shear under different earthquakes with PGA=0.55g



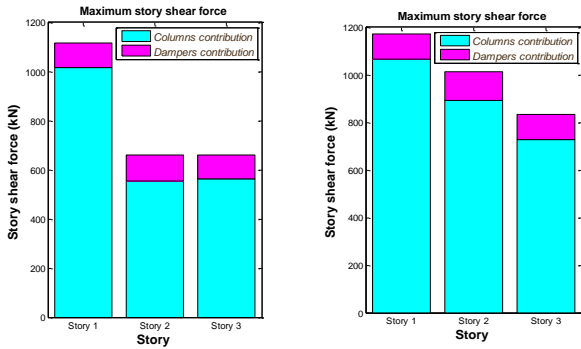
(c) Earthquake record: SE11 (d) Earthquake record: SE15
Figure 27 (cont'd). Maximum of columns shear under different earthquakes with PGA=0.55g



(c) Earthquake record: SE11 (d) Earthquake record: SE15
Figure 29. Contribution of columns and braces for resistance against shear forces under different earthquakes with PGA=0.35g

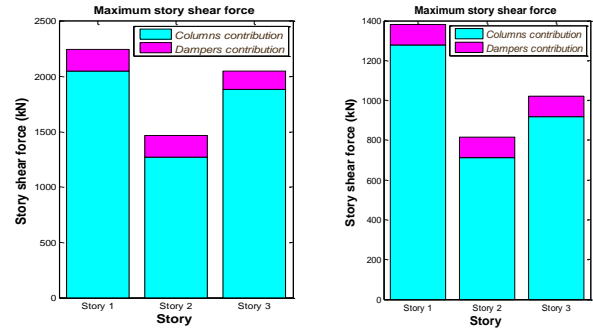


(a) Earthquake record: LA15 (b) Earthquake record: BO14

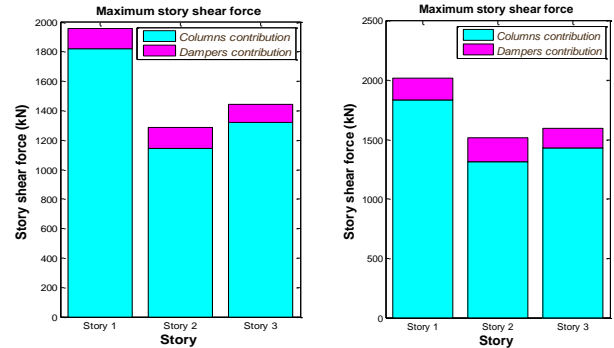


(c) Earthquake record: SE11 (d) Earthquake record: SE15

Figure 28. Contribution of columns and braces for resistance against shear forces under different earthquakes with PGA=0.20g

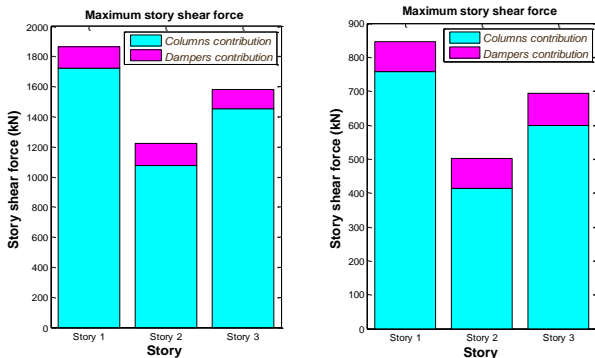


(a) Earthquake record: LA15 (b) Earthquake record: BO14



(c) Earthquake record: SE11 (d) Earthquake record: SE15

Figure 30. Contribution of columns and braces for resistance against shear forces under different earthquakes with PGA=0.55g



(a) Earthquake record: LA15 (b) Earthquake record: BO14

6. Issues and recommendations

It might be advisable to investigate additional types of dampers, such as concentrically bracing systems, eccentrically bracing systems, concrete frames, structures with concrete and steel shear walls, double systems, and other types of systems. The proposed numerical work can be extended to study the effect of other types of yielding dampers (TADAS dampers, ADAS dampers, BRB dampers, etc.) and the impact of each of these dampers on the behavior of bending moment frames.

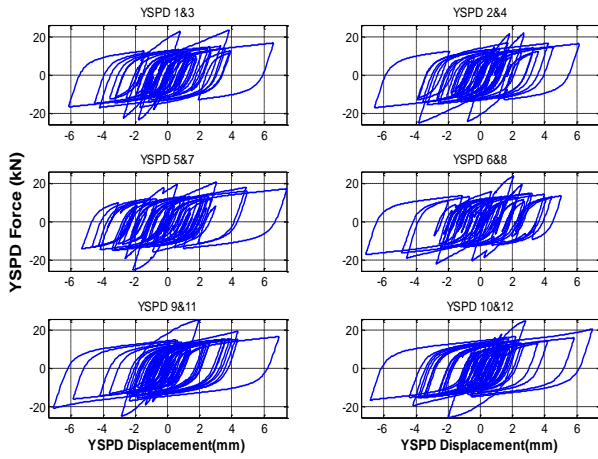


Figure 31. YSPD hysteresis loops of frame under BO14 earthquakes with PGA=0.20g

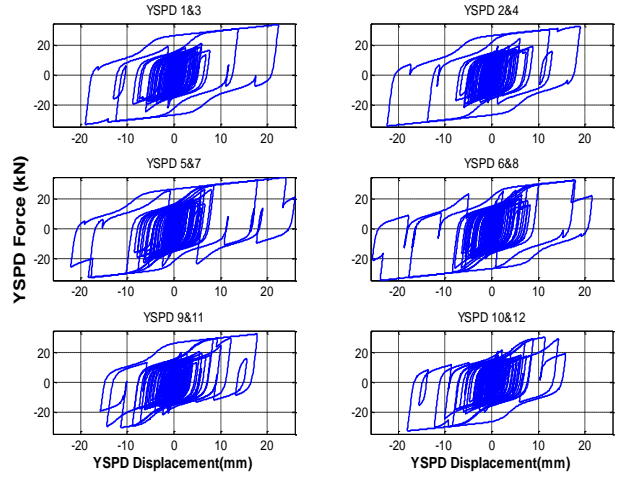


Figure 34. YSPD hysteresis loops of frame under SE11 earthquakes with PGA=0.20g

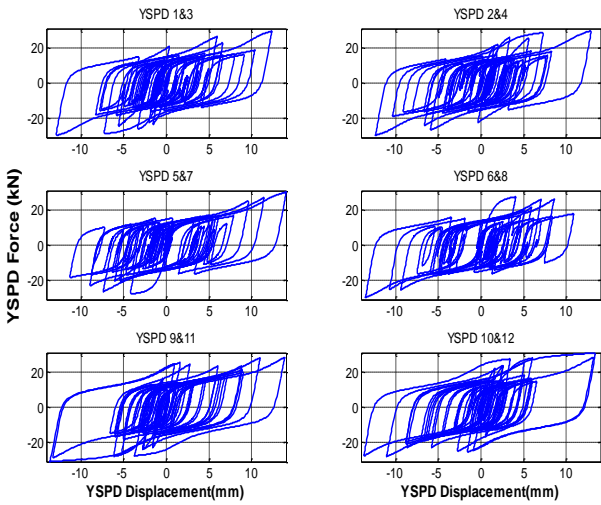


Figure 32. YSPD hysteresis loops of frame under BO14 earthquakes with PGA=0.35g

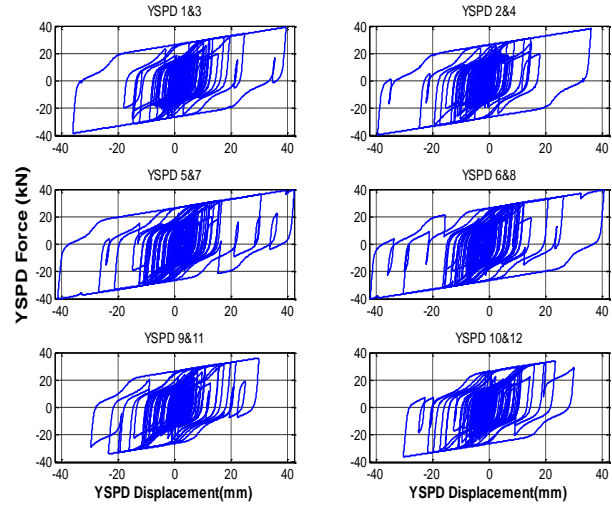


Figure 35. YSPD hysteresis loops of frame under SE11 earthquakes with PGA=0.35g

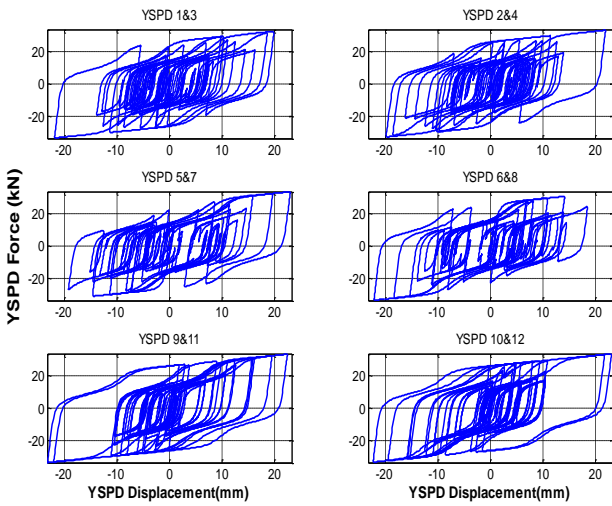


Figure 33. YSPD hysteresis loops of frame under BO14 earthquakes with PGA=0.55g

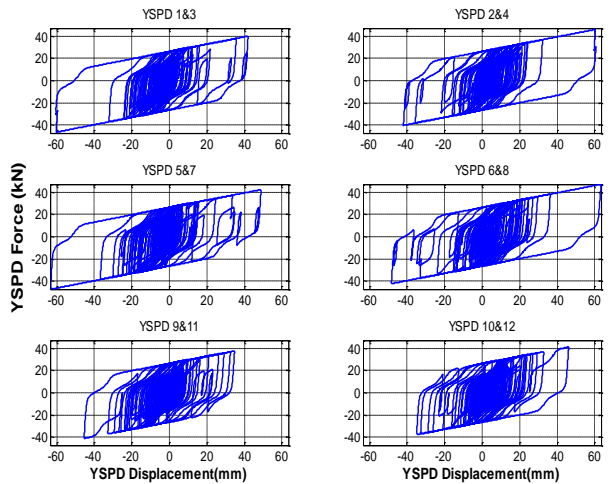


Figure 36. YSPD hysteresis loops of frame under SE11 earthquakes with PGA=0.55g

Also, the numerical work can be developed to investigate the effects of different heights, from short-rise buildings to tall buildings. Finally, the low-cycle fatigue performance in the software models and the simultaneous effect of dampers phenomenon can be investigated in the structures.

7. Conclusion

The following conclusions may be drawn based on the investigation's key findings:

- Using dampers has led to a significant reduction of drift in all stories of retrofitted frames during the time history response. Additionally, under varying earthquake intensities, the responses of the structures are nearly identical to each other.
- The second structure story recorded the most drifts, while the third story saw a decrease in drift value.
- The use of dampers has reduced total floor displacement. However, the effect of dampers on reducing displacement responses has been less than their effect on reducing drift responses. In all earthquake intensities, as the floor height increased, the amount of total displacement also increased.
- In most cases, the use of dampers has resulted in a reduction in the shear force of stories, and this use has had a positive effect on the time history of stories' shear force.
- In one earthquake record (LA15), the story shear force has increased in the first story, in other earthquake records, and in different earthquake intensities, the story shear force in the retrofitted frame has mostly decreased in contrast to the bare frame. While the reduction in story shear force is not statistically significant, it is nonetheless a significant improvement. The reason for this is that the use of yielding dampers (such as ADAS and TADAS dampers) mainly raises the stiffness of the structure and increases the absorption of more seismic force in the structures, and this is considered one of the disadvantages of using yielding dampers. However, one of the advantages of shear-yielding dampers is their ability to reduce the shear force of the stories.
- During the time history, at many times, the amount of shear force of the columns in the retrofitted frame was much lower than the amount of shear force of the bare frame, and therefore the dampers have performed well from this point of view.
- In all cases, a part of the shearing force has been absorbed by the braces, and this will reduce the contribution of the columns to absorb the shear forces. However, the dampers' contribution is not as significant as that of the columns. This is because the placement angle of the braces in the frame influences their behavior. Indeed, placing the braces more horizontally would enhance their ability to absorb shear forces. Therefore, we recommend placing the braces more horizontally and using them in larger spans. In another proposal, they could be implemented as concentrically X braces in the structure, which would reduce their angle to the horizon direction and improve their performance.
- Another important issue in evaluating dampers' performance is their hysteresis behavior. The result demonstrated that the used YSPD dampers effectively absorbed energy in all stories, and they also exhibited stable hysteresis loops, a crucial aspect of damper behavior. The area under these curves shows the energy absorbed by these dampers, and the larger area indicates that the damper has been able to dissipate a greater amount of seismic input energy.

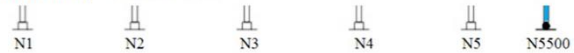
Appendix-A

A.1. Define seismic mass of nodes

```
# nodal coordinates:
node 1 0 0 0;
node 2 $LBeam 0 0; # node#, X, Y
node 3 [expr 2*$LBeam] 0 0;
node 4 [expr 3*$LBeam] 0 0;
node 5 [expr 4*$LBeam] 0 0;
node 6 0 $LCol -mass $mass1_ext $Usmall $Usmall;
node 7 [expr $LBeam] $LCol -mass $mass1_int $Usmall $Usmall;
node 8 [expr 2*$LBeam] $LCol -mass $mass1_int $Usmall $Usmall;
node 9 [expr 3*$LBeam] $LCol -mass $mass1_int $Usmall $Usmall;
node 92 [expr 3*$LBeam] $LCol -mass $mass1_ext $Usmall $Usmall;
node 10 [expr 4*$LBeam] $LCol -mass $mass1_ext $Usmall $Usmall;
node 102 [expr 4*$LBeam] $LCol -mass $mass2_ext $Usmall $Usmall;
node 11 0 [expr 2*$LCol] -mass $mass2_ext $Usmall $Usmall;
node 12 [expr $LBeam] [expr 2*$LCol] -mass $mass2_int $Usmall $Usmall;
node 13 [expr 2*$LBeam] [expr 2*$LCol] -mass $mass2_int $Usmall $Usmall;
node 14 [expr 3*$LBeam] [expr 2*$LCol] -mass $mass2_int $Usmall $Usmall;
node 142 [expr 3*$LBeam] [expr 2*$LCol] -mass $mass2_ext $Usmall $Usmall;
node 15 [expr 4*$LBeam] [expr 2*$LCol] -mass $mass2_ext $Usmall $Usmall;
node 152 [expr 4*$LBeam] [expr 2*$LCol] -mass $mass3_ext $Usmall $Usmall;
node 16 0 [expr 3*$LCol] -mass $mass3_ext $Usmall $Usmall;
node 17 [expr $LBeam] [expr 3*$LCol] -mass $mass3_int $Usmall $Usmall;
node 18 [expr 2*$LBeam] [expr 3*$LCol] -mass $mass3_int $Usmall $Usmall;
node 19 [expr 3*$LBeam] [expr 3*$LCol] -mass $mass3_int $Usmall $Usmall;
node 192 [expr 3*$LBeam] [expr 3*$LCol] -mass $mass3_ext $Usmall $Usmall;
node 20 [expr 4*$LBeam] [expr 3*$LCol] -mass $mass3_ext $Usmall $Usmall;
node 202 [expr 4*$LBeam] [expr 3*$LCol] -mass $mass3_ext $Usmall $Usmall;
```

A.2. Define of base column constraint

```
# Single point constraints -- Boundary Conditions
fix 1 1 1 1; # node DX DY RZ
fix 2 1 1 1; # node DX DY RZ
fix 3 1 1 1;
fix 4 1 1 1;
fix 5 1 1 1;
#fix base node
fix 5500 1 1 0; # node DX DY
```



A.3. Define gravity columns with p-delta effects

```
geomTransf PDelta 28;
#vertical elements
element elasticBeamColumn 12510 5500 10500 [expr 1000*9760*pow($in,4)] 200B6 [expr 18-6*9760*pow($in,4)] 28;
element elasticBeamColumn 18510 10500 15500 [expr 1000*9760*pow($in,4)] 200B6 [expr 18-6*9760*pow($in,4)] 28;
element elasticBeamColumn 24510 15500 20500 [expr 1000*9760*pow($in,4)] 200B6 [expr 18-6*9760*pow($in,4)] 28;
```

A.4. Define Hinges of beams

```
equalDOF 9 92 1 2
equalDOF 10 102 1 2
equalDOF 14 142 1 2
equalDOF 15 152 1 2
equalDOF 19 192 1 2
equalDOF 20 202 1 2
```



A.5. Define rigid Links

```
#truss elements
element truss 12500 10 10500 [expr 100*9760*pow($in,4)] 100;
element truss 18500 15 15500 [expr 100*9760*pow($in,4)] 100;
element truss 24500 20 20500 [expr 100*9760*pow($in,4)] 100;
```

Very stiff elastic material
Very large area

A.6. Define YSPD damper using BWBN material in Opensees

```
uniaxialMaterial material tag alpha X0 n gamma beta A q Zetas p Shi deltaShi Lambda tolerance maxNumberIter;
uniaxialMaterial BWBN 4 0.012331839 26.76 1.213 0.5 0.5 1 0.52 0.96 0.018 0.41 0.00001 0.0300 0.001 1000;
uniaxialMaterial BWBN 5 0.007746219 54.22 0.544 0.5 0.5 1 0.38 0.95 0.015 0.27 0.00001 0.0014 0.001 1000;
uniaxialMaterial BWBN 6 0.005240081 93.51 0.300 0.5 0.5 1 0.30 0.95 0.012 0.22 0.00001 0.0002 0.001 1000;
```

REFERENCES

[1] Whittaker AS, Bertero VV, Thompson CL, & Alonso LJ, Seismic Testing of Steel Plate Energy Dissipation Devices, Earthquake Spectra, 7 (4) , 365-

- 604 (1991). <https://doi.org/10.1193/1.1585644>
- [2] T.T. Soong B.F., & Spencer Jr, Supplemental energy dissipation: state-of-the-art and state-of-the-practice, *Engineering Structures*, 24, 3, 243-259 (March 2002). [https://doi.org/10.1016/S0141-0296\(01\)00092-X](https://doi.org/10.1016/S0141-0296(01)00092-X)
- [3] Tena-Colunga, Mathematical modelling of the ADAS energy dissipation device, *Engineering Structures*, 19, 10 (1997), 811-821. [https://doi.org/10.1016/S0141-0296\(97\)00165-X](https://doi.org/10.1016/S0141-0296(97)00165-X)
- [4] Tsai KC, & Hong CP., Steel triangular plate energy absorber for earthquake resistant buildings. In: *Constructional steel design: world developments*, Elsevier Applied, Science; (1992), 529-40.
- [5] Tehranizadeh M. Passive energy dissipation device for typical steel frame building in Iran. *Eng Struct*, 23(6) (2001), 643–55. [https://doi.org/10.1016/S0141-0296\(00\)00082-1](https://doi.org/10.1016/S0141-0296(00)00082-1)
- [6] Timler P, & Kulak GL. Experimental study of steel plate shear walls. *Structural Engineering Report No. 114*, Dept. of Civil Engineering, University of Alberta; 1983.
- [7] De Matteis G, Landolfo R, & Mazzolani FM. Seismic response of MR steel frames with low-yield steel shear panels. *Eng Struct*, 25(2) (2003), 155–68. [https://doi.org/10.1016/S0141-0296\(02\)00124-4](https://doi.org/10.1016/S0141-0296(02)00124-4)
- [8] Williams M, & Albermani F. Monotonic and cyclic tests on shear diaphragm dissipators for steel frames. *Adv Steel Constr*, 2(1) (2006), 1–21.
- [9] Chan RWK, Albermani F, & Williams MS. Evaluation of yielding shear panel device for passive energy dissipation. *J Constr Steel Res*, 65(2) (2009):260–8. <https://doi.org/10.1016/j.jcsr.2008.03.017>
- [10] Williams M, & Albermani F. Monotonic and Cyclic Tests on Shear Diaphragm Dissipators for Steel Frames. *Civil Engineering Bulletin No. 23*, Department of Civil Engineering, University of Queensland, Australia; 2003.
- [11] Schmidt K, Dorka UE, Taucer F, & Magnonette G. Seismic Retrofit of a Steel Frame and an Rc Frame with Hyde Systems. Institute for the Protection and the Security of the Citizen European Laboratory for Structural Assessment, European Commission Joint Research Centre; 2004.
- [12] Takahashi Y, & Shinabe Y. Experimental study of restoring force characteristics of shear yielding in thin steel plate elements. *J Struct Construct Eng*, 494, (1997):107–14 (in Japanese).
- [13] Md Raquibul Hossain, & Mahmud Ashraf, Mathematical modelling of yielding shear panel device, *Thin-Walled Structures*, 59 (2012) 153–161. <http://dx.doi.org/10.1016/j.tws.2012.04.018>
- [14] Kim TW, Wilcoski J, Foutch DA, & Leed MS. Shakedown tests of a cold-formed steel shear panel. *Eng Struct*, 28(10) (2006), 1462–70. <https://doi.org/10.1016/j.engstruct.2006.01.014>
- [15] Chan, R.W.K. Metallic Yielding Devices for Passive Dissipation of Seismic Energy, PhD Thesis, University of Queensland; 2008.
- [16] Chan, R.W.K., Albermani, F., & Kitipornchai, S., Experimental study of perforated yielding shear panel device for passive energy dissipation, 91 (2013), 14-25.
- [17] Maryam Salim. A , & Muhaned A. Shallal, Temperature change in steel-concrete composite bridge: Experimental and numerical study, *Al-Qadisiyah Journal For Engineering Sciences* 14 (2021) 117–127. <https://doi.org/10.30772/qjes.v14i2.760>.
- [18] Kareem Mohammed Alnebban , & Muhaned A. Shallal, Effect of filling steel tube chords by concrete on the structural behaviour of composite truss girders, *Al-Qadisiyah Journal For Engineering Sciences* 13 (2020) 167–174. <https://doi.org/10.30772/qjes.v13i3.662>.
- [19] Hossain, M. R., Ashraf, M., & Albermani, F., Numerical evaluation of yielding shear panel device: a sustainable technique to minimize structural damages due to earthquakes, *Universitas 21 International Graduate Research Conference: Sustainable Cities for the Future*, (2009), pp: 65-68.
- [20] Li Zhengying, Faris Albermani, Ricky W.K. Chan, & S. Kitipornchai, Pinching hysteretic response of yielding shear panel device, *Engineering Structures*, 33 (2011), 993-1000. <https://doi.org/10.1016/j.engstruct.2010.12.021>
- [21] Md Raquibul Hossain, & Mahmud Ashraf, Mathematical modelling of yielding shear panel device, *Thin-Walled Structures*, 59 (2012) 153–161. <http://dx.doi.org/10.1016/j.tws.2012.04.018>.
- [22] Hossain MR, Ashraf M, & Albermani F. Numerical modelling of yielding shear panel device for passive energy dissipation. *Thin-Walled Struct*, 49(8) (2011), 1032–44. <https://doi.org/10.1016/j.tws.2011.03.003>.
- [23] Li Z et al. Pinching hysteretic response of yielding shear panel device. *Eng Struct*, 33(3) (March 2011), 993-1000. <https://doi.org/10.1016/j.engstruct.2010.12.021>.
- [24] Hossain MR, Ashraf M. Mathematical modelling of Yielding Shear Panel device. *Thin-Walled Struct*, 59 (2012) :153–61. <https://doi.org/10.1016/j.tws.2012.04.018>.
- [25] Ellingwood BR, & Kinali K. Quantifying and communicating uncertainty in seismic risk assessment. *Struct Saf*, 31(2) (2009):179–87. <https://doi.org/10.1016/j.strusafe.2008.06.001>.
- [26] FEMA, 355-C: State of the art report on systems performance of steel moment frames subject to earthquake ground shaking. Federal Emergency Management Agency, Washington, DC; 2000.
- [27] Ohtori Y, & Spencer Jr B., Benchmark control problems for seismically excited nonlinear buildings, *J Eng Mech*, (2004),130:366.
- [28] Walter.Yang CS, DesRoches R, & Leon RT., Design and analysis of braced frames with shape memory alloy and energy-absorbing hybrid devices, *Eng Struct*, 32(2) (2010), 498–507. <https://doi.org/10.1016/j.engstruct.2009.10.011>
- [29] Bitaraf M, Hurlebaus S, & Barroso LR., Active and semi active adaptive control for undamaged and damaged building structures under seismic load, *Comput Aided Civil Infrastruct Eng*, (2011). <https://doi.org/10.1111/j.1467-8667.2011.00719.x>
- [30] Ozbulut OE, Hurlebaus S. Seismic control of nonlinear benchmark building with a novel re-centering variable friction device. In: *Ninth Pacific conference on earthquake engineering*, Auckland, New Zealand; 2011.
- [31] Christenson R et al. Large-scale experimental verification of semiactive control through real-time hybrid simulation. *J Struct Eng* 134(4) (2008), 522–34.
- [32] Mazzoni S, McKenna F, & Fenves GL. *OpenSees command language manual*. Pacific Earthquake Engineering Research (PEER) Center; (2005).
- [33] Hossain, M. R., Ashraf, M., Padgett, J. E., Probabilistic seismic performance evaluation for yielding shear panel design, *Australasian Structural Engineering Conference The past, present and future of Structural Engineering*. Barton, A.C.T.: Engineers Australia, (2012), 58-65.
- [34] Baber, T. & Noori, M., Modelling general hysteresis behavior and random vibration application, *J Vib Acoust Stress Reliab Des*, (1986), 411-20.
- [35] Hossain, M. R., Asraf, M., & Padgett, J.E., Risk-based seismic performance assessment of Yielding Shear Panel Device, *Engineering Structures*, 56 (2013), 1570-1579.
- [36] Chen Xuewei, Han Xiaolei, Jack CHEANG, Lin Shengyi, & Mao Guiniu, Dynamic Inelastic Numerical Simulation for a Shaking Table Test of a Full-Scale Steel Moment Frame Structure based on OpenSEES, *The 14 th World Conference on Earthquake Engineering* October (2008), 12-17, Beijing, China.
- [37] Scott, M. H. & Fenves, G. L., Plastic hinge integration methods for force-based beam-column elements., *J Struct Eng*, (132) (2006), 244-252.